Reactions under Autogenic Pressure at Elevated Temperature (RAPET) of Various Alkoxides: Formation of Metals/Metal Oxides-Carbon Core-Shell Structures

Swati V. Pol, Vilas G. Pol, and Aharon Gedanken*[a]

Abstract: The RAPET reaction at 700 °C, of different alkoxides (Ti, V, and Si) led to three different nanocomposites. Carbon is the element common to all three structures. Carbon was found as the core in the decomposition of TEOS, as the shell in the decomposition of $VO(OEt)_3$ and embedded in, or mixed completely with, TiO_2 in the decomposition of $Ti(OiPr)_4$. This novel method using only metallic alkoxide precursor, in the absence of catalyst, leads in a one-step process to core-shell structures.

Keywords: carbon · chemical vapor deposition · core-shell structures · high-pressure chemistry · RAPET reaction

Introduction

Titanium dioxide is a most important photocatalyst, especially for the detoxification of air and water. Many projects have focused on the preparation, as well as on the modification,[1,2] of TiO_2. Some of these have reported the preparation of composites containing TiO_2 and carbon.[3] Photocatalyst anatase-type TiO_2 particles were coated with a carbon layer by mixing them with poly-vinyl alcohol and then heating above 700 °C under a N_2 gas flow. The presence of carbon layers on the TiO_2 particles was found to be beneficial to their photocatalytic activity, suppressing the phase transformation of anatase to the rutile structure by preventing sintering and crystal growth.[4] TiO_2-mounted activated carbon has been prepared by the precipitation of TiO_2 from tetraisopropyl orthotitanate on the surface of poly(vinyl butyral) (PVB) and subsequent carbonization to different temperatures, from 700 to 900 °C, under a flow of carbon dioxide.[5] Photostable catalysts for visible light degradation of 4-chlorophenol have been obtained by the simple calcination of an alcoholic suspension of titanium dioxide. The catalysts show an excellent long-time stability, which indicates either that the active sites themselves are resistant to photochemical degradation or they are regenerated during the degradation of the pollutants. The observed generation of a photocurrent supports the postulation of an electron transfer from the sensitizer (coke) to the conduction band[6] of the TiO_2. It has been reported that the addition of activated carbon to titania slurry could increase the decomposition of some organic compounds in the photocatalytic process.[7] Fine particles of photocatalytic anatase-type TiO_2, prepared by hydrolysis of titanium-tetraisopropoxide, were coated with carbon by precipitation in a polyvinyl alcohol (PVA) aqueous medium, followed by heat treatment at temperatures of 400–1000 °C in a flow of high purity Ar.[8] The preparation of carbon coated[9] Al_2O_3, carbon-coated[10] SiO_2, carbon-coated[11] MgO nanoparticles, and carbon-coated SiO_2, Al_2O_3, ZrO_2 and TiO_2 materials[12] has also been reported.

Silicon is widely used in transistors, solar cells, rectifiers, computer chips, lubricants, and other electronic devices. Recently, several research groups employed the laser ablation method for the fabrication of silicon nanoparticles.[13–16] A number of research articles emphasize SiO_2 deposition on several substrates by pyrolyzing[17] TEOS. TEOS has become popular as a single source precursor for SiO_2 since it has many desirable properties, and oxides of high quality can be produced by its pyrolysis at a relatively low deposition temperature.[18] SiO_2 has been used extensively in large integrated circuits, such as bipolar and metal oxide semiconductor devices, because of its unique electrical and mechanical properties as an insulator. The films[19]deposited by TEOS (Tetraethylorthosilicate) are also utilized in protective layer coatings, electronic sensors, chemically modified electrodes, thin film optics, and antireflection coating.

V_2O_3 powder is also used in conductive polymer composites and in catalysts.[20] The synthesis of spherical V_2O_3 nanoparticles by the reductive[20] pyrolysis of ammonium oxovanadium(IV) carbonato hydroxide has been reported. Thermal decomposition of divanadium pentoxide[21] was carried out by Su et al. to synthesize nanocrystalline V_2O_3.

[a] S. V. Pol, V. G. Pol, Prof. A. Gedanken
Department of Chemistry, Bar-Ilan University
Ramat-Gan, 52900 (Israel)
Fax: (+972) 3-5351250
E-mail: gedanken@mail.biu.ac.il

 DOI: 10.1002/chem.200400014

In this article we report on an efficient method that uses a single precursor, a metallic alkoxide, and in one step produces core-shell structures of metals/metal oxides with carbon. The reactions are conducted without a catalyst. These types of reactions are divided into three classes. In the first, the thermal decomposition of $Ti[OCH(CH_3)_2]_4$ produces titania embedded in carbon (TEC), and the fabricated carbon cannot be separated from anatase titania. In the second, the thermal decomposition of $VO(OC_2H_5)_3$ produces carbon coated vanadium oxide (CCVO), where the obtained nanosized V_2O_3 is the core and the carbon is produced as a uniform shell. In the third category, the thermal decomposition of $Si(C_2H_5O)_4$ produces silicon coated carbon spheres (SCCS). The carbon is produced as a spherical core and Si forms a nanoshell. Interestingly while all three alkoxide reactions were separately carried out for the same heating period in a closed Swagelok cell at 700 °C, they led to morphologically and structurally different products.

Results and Discussion

Here we present and compare results related to various metal alkoxides that produces core-shell structures of metals/metal oxides with carbon. The carbon and hydrogen content in the product/carbonaceous materials was determined by elemental analysis measurements. The calculated element percent of carbon in $Ti[OCH(CH_3)_2]_4$, $VO(OC_2H_5)_3$ and $Si(C_2H_5O)_4$ are 50.7, 44.3, and 46%, while the element percent of hydrogen are 9.8, 9.6, and 8.6%, respectively. The measured percent of carbon in TEC, CCVO and SCCS products are 34, 30, and 22%, while the percent of hydrogen are 0.6, 0.3, and 0.6%, respectively. It is obvious that the products show less carbon than the reactants, while the percent of hydrogen is almost negligible. This means that some of the carbon is used for the reduction of the reactants and/or bonded to hydrogen in the form of hydrocarbons. Furthermore, the reduction of the transition metal is observed in both the CCVO and the SCCS products. This reduction might have occurred due to the carbon acting as a reducing agent at high temperatures.

The XRD pattern of the as-prepared TEC sample is presented in Figure 1a. The diffraction peaks were observed at $2\theta = 25.3$, 37.9, 48.15, 54.05, and 55.2°, and are assigned as (101), (004), (200), (105), and (211) reflection lines of the body centered tetragonal phase of TiO_2. These values are in good agreement with the diffraction peaks, peak intensities and cell parameters of crystalline anatase TiO_2 (PDF No. 73-1764). Another important observation attributed to the carbon coating is the suppression of phase transformation from anatase to rutile. The products of the RAPET reactions at 700 and 900 °C show an anatase titania phase as evidenced by XRD. The anatase phase is formed below 500 °C and ordinarily starts to transform[8] to a rutile-type structure above 600 °C. Since, in the TEC the amount of carbon coating is high (34 wt.%), it prevents the change of the anatase phase to rutile. Therefore, the carbon coating suppressed the phase transformation from anatase to rutile. Similar results were recently reported by Inagaki et al.[4] They found

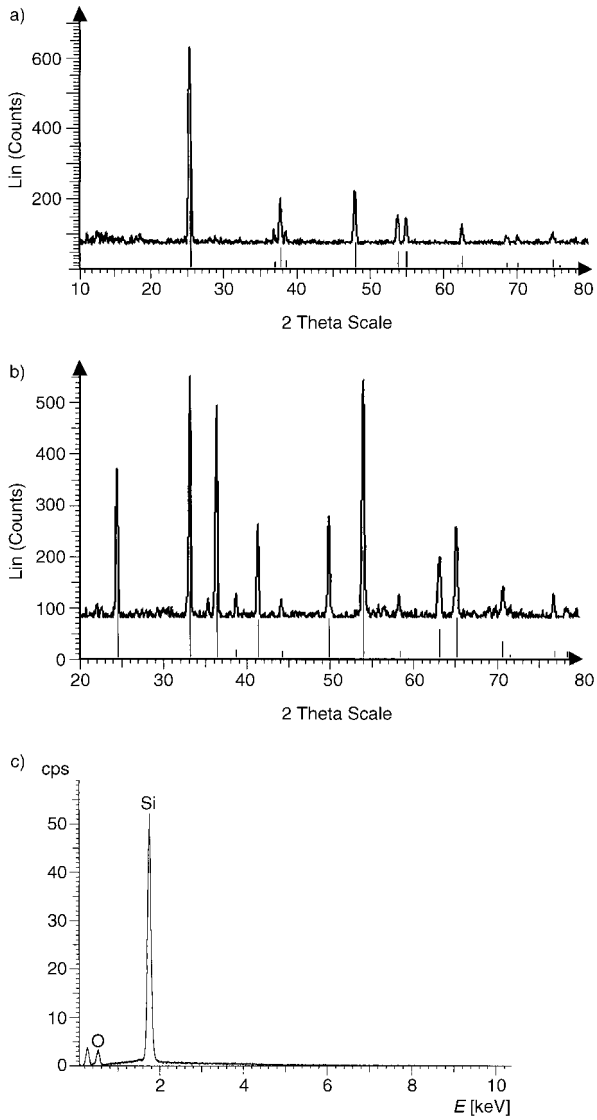

Figure 1. a) Powder XRD pattern of TEC product b) Powder XRD pattern of CCVO product. c) Energy dispersive X-ray analysis of the SCCS sample.

that the minimal amount of coated carbon for the suppression of phase transformation is about 5 mass%. This is a threshold[8] level for this phenomenon.

The XRD pattern of the as-prepared CCVO sample is presented in Figure 1b. Diffraction peaks were observed at $2\theta = 24.3$, 33,0, 36.3, 38.5, 41.2, 49.8, 53.9, 63.2, 65.2, and 70.7°, and are assigned as (012), (104), (110), (113), (024), (116), (214), (300) and (1010) reflection lines of the Rhombohedral V_2O_3 phase. These values are in good agreement with the diffraction peaks, peak intensity and cell parameters of crystalline V_2O_3 (PDF No. 74-325). The Scherrer equation is used to calculate the particle dimensions,[22] and the average particle size of TiO_2 and V_2O_3 is ~50 nm. No peaks characteristic of carbon were observed in CCVO and TEC samples, and this might be due to their amorphous nature.

Since the SCCS sample is XRD amorphous, the composition of Si and O in the SCCS sample is detected by EDX

(Figure 1c). The results show that the molar ratio of Si/O is 59:40 (1:0.67) in the SCCS sample. The percentage of oxygen is thus insufficient for SiO or SiO_2 in the SCCS sample. It is well known that bare Si is highly sensitive to air, and the surface of the Si nanoparticles might be oxidized. The small signal on the left side is that of carbon.

Microscopic measurements: The morphology of all the samples was studied by TEM measurements. For TEC the image (Figure 2a) depicts nanoparticles of anatase titania homogeneously embedded in carbon. We assume that the dissociation of $Ti[OCH(CH_3)_2]_4$ at 700 °C, leads to dissociation into carbon, hydrogen, oxygen and titanium atoms, or carbon, hydrogen, and titania. If the former reaction occurs, then the titanium and oxygen atoms react and lead to the formation of a spherical anatase TiO_2 that mixes with the carbon under cooling. The diameter of these TiO_2 nanoparticles is in the range of 25–50 nm and has the tendency to form a bulk of 30–40 nanoparticles surrounded by carbon [Figure 2a]. The pictures at higher magnification show that the anatase TiO_2 (Figure 2b) is densely embedded in carbon. The image taken at the edge of the TEC sample showed disordered, coal-like lattice planes of the amorphous carbon, which could not be detected in the XRD measurements. The HR-TEM depicted in Figure 2c provides further evidence for the identification of the product as TiO_2. The image is recorded along the [101] zone. It illustrates the perfect arrangement of the atomic layers and the lack of defects. The measured distance between these (101) lattice planes is 0.352 nm, which is very close to the distance between the planes reported in the literature (0.351 nm) for the body centered tetragonal lattice of the TiO_2 (PDF: 73-1764).

The morphology of the CCVO sample was studied by TEM measurement. It shows spherical particles coated with a nanolayer of a contrasting material. As in the above proposals, we assume that the dissociation of $VO(OC_2H_5)_3$ at 700 °C leads either to dissociation into carbon, hydrogen, oxygen and vanadium atoms, or to the immediate formation of V_2O_5. In the former case the vanadium and oxygen atoms react and lead to the formation of a spherical V_2O_3 core molecule and a smooth shell of carbon under cooling. In the latter case the V_2O_5 further react with carbon to yield V_2O_3. The diameters of these cores range between 30 and 100 nm (Figure 3a). It is worth mentioning that the core size can be varied but the carbon shell is always constant (~15 nm). This uniform 15 nm shell helps to stabilize the core and does not allow a change in the oxidation state neither at room temperature, nor when heated in water for 2 d. All the V_2O_3 nanoparticles are uniformly coated with a carbon shell. The picture at higher magnification shows that the V_2O_3 core (Figure 3b) is densely decorated with uniform carbon shells of ~15 nm. The image taken at the edge of the CCVO sample showed disordered lattice planes of carbon (Figure 3c). These disordered layers correspond to the non-graphitic, coal-like lattice planes of the carbon, which could not be detected in XRD measurements. The interlayer spacing is ~3.8 Å, which is larger than the graphitic layers. The HR-TEM is depicted in Figure 3d and provides further verification for the identification of the core as V_2O_3. The image is recorded along the [104] zone. It illustrates the perfect arrangement of the atomic layers and the lack of defects. The distance measured between these (111) lattice planes is 0.273 nm, which is very close to the distance between the

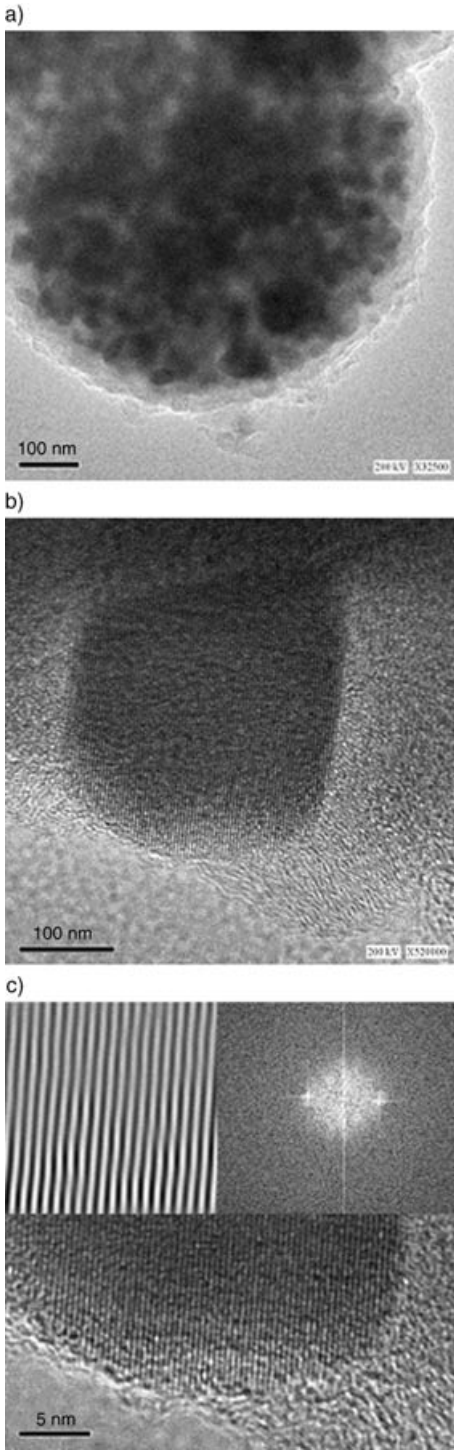

Figure 2. Transmission electron micrographs of a) anatase titania embedded in carbon, b) anatase titania at high resolution and c) perfect atomic layers arrangements of TiO_2 along [101] zone axis. Inserts: left upper corner: Fast Fourier Transform filtered image of the lattice, and to the right, computer generated diffraction pattern of the same lattice image.

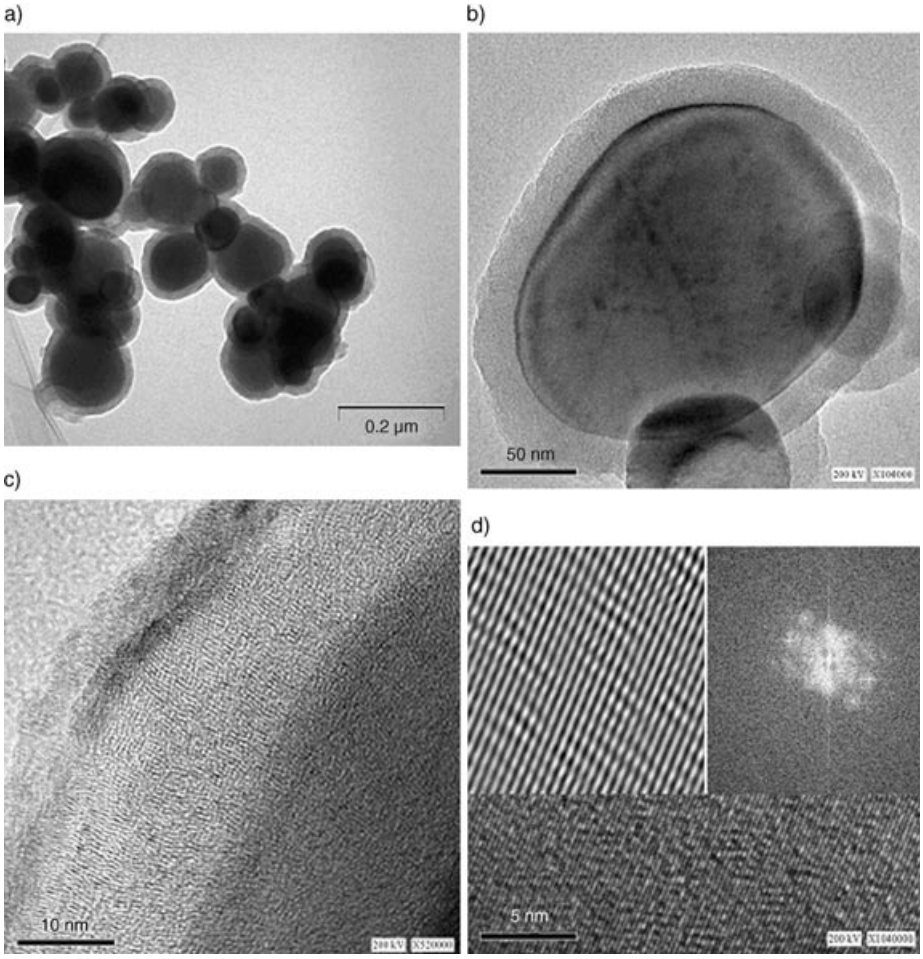

Figure 3. Transmission electron micrographs of a) CCVO sample, b) single particle of CCVO at high resolution, c) carbon shell marked by an arrow, d) perfect atomic layer arrangements of V_2O_3 along [104] zone axis (Inserts: Left upper corner: Fast Fourier Transform filtered image of the lattice, and to the right, computer generated diffraction pattern of the same lattice image).

planes reported in the literature (0.271 nm) for the rhombohedral lattice of the V_2O_3 (PDF: 74-325).

The decomposition of $Si(C_2H_5O)_4$ in a closed Swagelok cell at 700 °C produced an X-ray amorphous product. Even though the sample was prepared at 700 °C, we have tried to crystallize the product by heating up to 1100 °C in an inert atmosphere, but failed to obtain any XRD diffraction patterns. Therefore, a systematic analysis was carried out to characterize the amorphous product. The morphology of the SCCS sample was studied by TEM measurement. It depicts spherical particles coated with contrasting nanoparticles. We assume that the dissociation of TEOS at 700 °C leads to a complete dissociation into carbon, hydrogen, oxygen, and silicon atoms. These carbon atoms lead to the formation of spherical carbon cores under cooling. The boiling point of carbon (4200 °C) is much higher than that of silicon (2355 °C). After dissociation at 700 °C, and subsequent cooling, the preferred solid-state form of carbon is the spherical form. Silicon is then deposited on these formed carbon spherules (CSs). This implies that carbon solidifies first, both thermodynamically and kinetically. The diameter of these cores ranges between 0.3 and 1 μm. The formation of spherical carbon is confirmed by microtoming these spheres. To determine whether the spherical body is a solid carbon body rather than a hollow sphere, a dry powder is immersed in epoxy plastic (according to Spurr's formulation) and put into a capsule to harden. The hard blocks are cut using an LKB ultratome III, and the ultra thin sections are placed on bare 400 mesh copper grids for TEM measurement of the spherule's cross-section (Figure 4c). SAEDS was determined on an individual spherule cross section, which confirmed that the core of the spherical body is composed of carbon only, exhibited as a strong carbon peak. This peak was much stronger than that of the carbon peak originating from the TEM grid. Transmission electron microscopy images of the silicon coated carbon sphere products unambiguously revealed that the diameter/thickness of the silicon layer is ~15 nm. The SAEDS employed on the edge of the carbon spheres with a 15 nm electron beam detected only the presence of Si and oxygen. The percentages of Si, and O are 85 and 15, respectively. This very small amount of oxygen might be due to the surface oxidation of Si during sample preparation. In the SCCS sample (Figure 4a), Si nanoparticles are anchored on the outer surfaces of the CSs, and in some places they aggregate and pile up on the surface of the CSs. Most of the CSs are decorated with Si nanoparticles. Some homogeneous excess Si nanoparticles are also observed (indicated by an arrow) in the SCCS sample. The pictures at higher magnification show that the CSs (Figure 4b) are densely decorated with uniform Si nanoparticles whose diameters are less than 15 nm. Due to the amorphous nature, no fringes were observed in HR-TEM attributed to the interplane distances of the C or Si atoms (Figure 1d). XPS results also support our claim that the shell is composed primarily of silicon.

The measured surface areas for the TEC, CCVO, and SCCS products are 16, 27, and 150 $m^2 g^{-1}$, respectively. The high surface area of the SCCS product is due to the mesoporous Si that is coated on the surface of the carbon sphere. The CCVO, SCCS and TEC products (carbonaceous compounds), after heating at ~500 °C in an air atmosphere, produce pure V_2O_5, amorphous silica, and anatase titania, respectively, as confirmed by XRD and EDX.

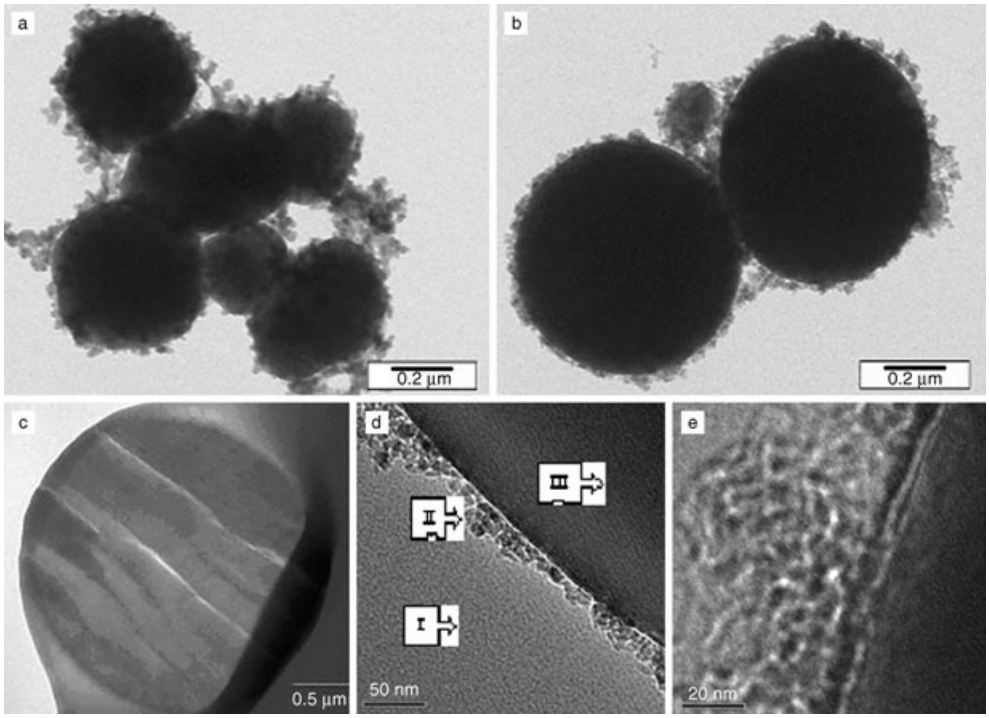

Figure 4. Transmission electron micrographs of a) SCCS sample; b) SCCS at high resolution; c) spherule's cross-section and d) HRTEM images of SCCS sample: I) Carbon background of TEM grid, II) Si nanoparticles, and III) spherical carbon; e) HR-TEM of SCCS sample shows the porous nature of coated Si nanoparticles. The bar measures 20 nm.

The core-shell composite structures of metals/metal oxides/carbon were found to be of three different types. Raman spectroscopy measurements were performed to understand the nature of the carbon in the CCVO, TEC, and SCCS samples. The micro-Raman spectra of CCVO (a), SCCS (b) and TEC (c) samples are shown in Figure 5. The two characteristic bands of carbon were detected at 1340 cm^{-1} (D band), and at 1595 cm^{-1} (G band).[23] The intensity ratios of the D and G bands were: $I_D/I_G = 1.1$, 0.6 and 0.5 for the CCVO, SCCS, and TEC samples, respectively. An increase in the intensity of the G peak associated with graphitic carbon is observed for the SCCS and TEC samples. On the other hand, the CCVO sample shows an increase in the intensity of the D peak associated with disordered carbon. It is suggested that the existence of the non-graphitic layers is due to the execution of the RAPET reaction at a temperature (700 °C), which is not high enough to permit improvement of the local order of the deposited carbon.

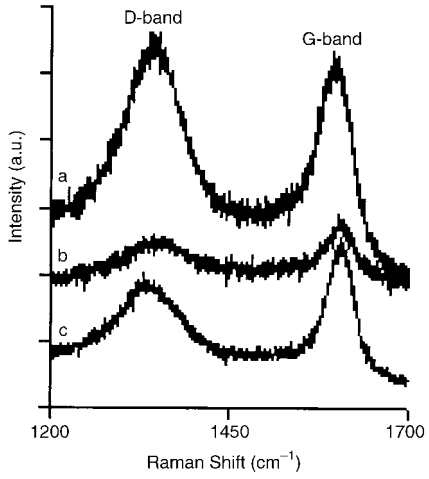

Figure 5. Raman spectra of CCVO (a), SCCS (b) and TEC (c) samples.

To probe the gaseous products of the RAPET reaction of $VO(OC_2H_5)_3$ we have assembled a system which can detect pressure inside the Swagelok, and can be directly attached to the mass spectrometer for analyzing the gases formed in the decomposition. The residual gas pressure at the end of the reaction, after cooling the Swagelok, is very small (< 2 atm). Peaks at 18, 28, 44 amu were observed in the mass spectrum. The signal at 18 amu is assigned to water. The mass of 28 can be attributed to either nitrogen (the cell was filled under nitrogen) or to CO originating from the dissociation of CO_2 under the electron bombardment. The mass of 44 is due to C_3H_8, or CO_2, or to both. (Equation 1) Based on XRD, HR-TEM, and CHNS analysis, and on mass spectrometry results for the CCVO sample, the following reaction is suggested. The calculated element percent of carbon in $VO(OC_2H_5)_3$ was 44.3 while 30% carbon is found in the CCVO product. Here, ~15 wt% of carbon is lost in the reaction as CO_2 and gaseous hydrocarbons (see Table 1).

$$2\,VO(OC_2H_5)_3 \xrightarrow{700^{\circ}C} V_2O_3 + 8\,C + CO_2 + C_3H_8 + 3\,H_2O + 8\,H_2$$

It appears that in the RAPET reactions of mesitylene and TEOS complete dissociation[24] (breaking all C–C and C–H bonds) into carbon and hydrogen (mesitylene), and into

Table 1. Reactants, products, and characteristic properties.

Compounds	$VO(OC_2H_5)_3$	Si $(C_2H_5O)_4$	$Ti[OCH(CH_3)_2]_4$
products	CCVO	SCCS	TEC
TEM observations	$C@V_2O_3$	Si@C	TiO_2-C
XRD measurements	V_2O_3	amorphous	TiO_2 anatase
BET surface area $[m^2g^{-1}]$	27	150	16
melting point [°C][a]	V_2O_3 2067 C 3727	Si 1410 SiO_2 1722	TiO_2 1843
boiling point [°C][a]	V_2O_3 3450 C 4200	Si 2355 SiO_2 2950	TiO_2 2500–3000
element %			
carbon, reactant [%]	44.3	46	50.7
product [%]	30	22	34
hydrogen, reactant [%]	8.6	9.6	9.8
product [%]	0.6	0.3	0.6

[a] Melting and boiling points in *Handbook of Chemistry and Physics* (Ed.: D. R. Lide), 82 ed., **2001–2002**.

carbon, hydrogen, oxygen and silicon atoms (TEOS)[25] takes place, while in the RAPET reactions of the transition metal ethoxides the V–O, and Ti–O bonds are not broken. All the products of the dissociation reaction float in the gas phase and solidify right after their formation. The question is what solidifies first and what determines the order of the solidification. While for TEOS we can account for the solidification of the carbon as the core sphere, both thermodynamically and kinetically, the other results can be explained only on a kinetic basis. Because the boiling and melting points of carbon are much higher than those of the transition-metal oxides, carbon would therefore tend more to become a solid at 700 °C. In other words from the thermodynamic point of view carbon would be the first to solidify and form the core and the V_2O_3 would create the shell. However, since the process is kinetically controlled the opposite is occurring. Namely, V_2O_3 has a much higher solidification rate than carbon to form the core of the composite. Carbon, having a slower solidification rate, forms the shell layer. In the RAPET reaction of TEC the solidification rates of TiO_2 and carbon are almost equal and they form a homogeneous alloy-like composite.

Our mechanism is based on CVD results that were usually obtained at lower temperatures. It is therefore safe to assume either the complete dissociation or the fragmentation to the metal oxide from the corresponding alkoxides. For example, similar investigations[26–28] on dissociation or precursor's fragmentation are reported. Using a Ni-Sn heterometal alkoxide, $[Ni_2Sn_2(O'Bu)_8]$, in a chemical vapor deposition (CVD) process. Fragmentation of the precursor[26] and disproportionation of the tin(II) component dominate up to 500 °C, and results in the formation of NiO, Sn^0, and SnO_2. Metallorganic chemical vapor deposition of Ta_2O_5 films is reported[27] by using Tantalum(v) ethoxide, since its decomposition temperature is low. Films of Ta_2O_5 were grown in the temperature range 400–800 °C. Metal-organic CVD of titanium(IV) neo-pentoxide, and zirconium(IV) neo-pentoxide precursors, were found to possess relatively high volatility at 330 and 160 °C, respectively, to produce titania and zirconia.[28]

In conclusion, the novel one-step RAPET reactions at 700 °C of various metal alkoxides in the absence of catalyst led to three different types of core shell composites. Carbon is the common element to all three structures. Carbon, was found as the core in the decomposition of TEOS, as the shell in the decomposition of $VO(OEt)_3$ and embedded or mixed completely with TiO_2 in the decomposition of titanium isopropoxide.

Experimental Section

Preparation of core shell structures of metals/metal oxides with carbon from various alkoxides: Vanadium(v) oxytriethoxide $[VO(OC_2H_5)_3$, (95 %)], tetraethlyorthosilicate [TEOS, $Si(C_2H_5O)_4$, (99 %)] and titanium(IV) isopropoxide $[Ti[OCH(CH_3)_2]_4$, 99 %], were purchased from Aldrich and used without further purification. The preparation of the core shell structure of metals/metal oxides with carbon from these alkoxides is carried out in a 5 mL closed cell. The cell is assembled from stainless steel Swagelok parts. A $^1/_2''$ union part is plugged on both sides by standard caps as shown in Figure 6. For these syntheses, 2 g of one of the

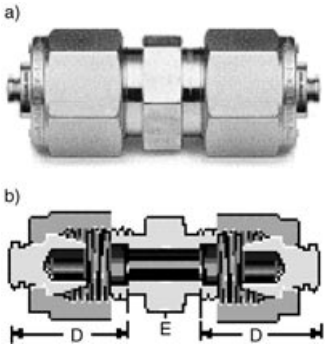

Figure 6. a) An overview of the Swagelok used for the RAPET reaction and b) cross-section of the Swagelok; D: cap, E: union.

above precursors are introduced into the cell at room temperature under nitrogen (a nitrogen filled glove box). The filled cell is closed tightly with the other plug and then placed inside an iron pipe in the middle of the furnace. The temperature is raised at a rate of 10 °C per minute. The closed vessel cell is heated at 700 °C for 1 h. The reaction proceeds at an autogenic pressure of the precursor. The Swagelok is gradually cooled (~5 h) to room temperature, opened with the release of a little pressure, and a dark black powder is collected. We termed this synthesis process as "Reaction under autogenic pressure at elevated temperatures" (RAPET). The total yield of product/carbonaceous material is about 55 % for TEC, 29 % for CCVO, and 38 % for SCCS. All yields are relative to the weight of the starting materials. All the products are characterized by structural and morphological techniques.

Instrumental: XRD patterns were collected by using a Bruker AXS D* Advance powder X-Ray diffractometer ($Cu_{K\alpha}$ radiation, wavelength 1.5406 Å). The morphologies and nanostructure of the as-synthesized products were further characterized with a JEM-1200EX TEM and a JEOL-2010 HRTEM using an accelerating voltage of 80 and 200 kV, respectively. SAEDS (Selected Area Energy Dispersive X-ray Analysis) of one individual particle was conducted using a JEOL-2010 HRTEM model, and EDX by using an X-ray microanalyzer (Oxford Scientific), both attached to a JSM-840 scanning electron microscope (SEM). Samples for TEM and HRTEM were prepared by ultrasonically dispersing the products into absolute ethanol, placing a drop of this suspension onto a copper grid coated with an amorphous carbon film, and then drying in air. Specific surface areas were measured by the Brunaur–Emmett–Teller (BET) method at 77 K using N_2 gas as an absorbent after heating the

sample at 100 °C for 1 h. The elemental analysis of the samples was carried out by an Eager 200 C, H, N, S analyzer. The Olympus BX41 (Jobin Yvon Horiba) Raman spectrometer was employed, using the 514.5 nm line of an Ar laser as the excitation source to analyze the nature of the carbon present in TEC, CCVO, and SCCS products. For the analysis of the residual gases in the reaction cell, the FAB^+ mass spectra were recorded on a VG Autospec (Fisons Instruments).

Acknowledgement

The authors would like to thank to Prof. Z. Malik, Department of Life Sciences, for extending the use of LR-TEM facility. This research article is a part of S.V. Pol's Ph.D. work.

[1] J. C. Yu, J. G. Yu, J. C. Zhao, *Appl. Catal. B* **2002**, *36*, 31 – 43.
[2] V. G. Pol, R. Reisfeld, A. Gedanken, *Chem. Mater.* **2002**, *14*, 3920 – 3924.
[3] T. Tsumura, N. Kojitani, H. Umemura, M. Toyoda, M. Inagaki, *Appl. Surf. Sci.* **2002**, *196*, 429 – 436.
[4] T. Tsumura, N. Kojitani, I. Izumi, N. Iwashita, M. Toyoda, M. Inagaki, *J. Mater. Chem.* **2002**, *12*, 1391 – 1396.
[5] B. Tryba, A. W. Morawski, M. Inagaki, *Appl. Catal. B* **2003**, *46*, 203 – 208.
[6] C. Lettmann, K. Hildenbrand, H. Kisch, W. Macyk, W. F. Maier, *Appl. Catal. B* **2001**, *32*, 215 – 227.
[7] J. Matos, J. Laine, J. M. Hermann, *J. Catal.* **2001**, *200*, 10 – 20.
[8] M. Inagaki, Y. Hirose, T. Matsunaga, T. Tsumura, M. Toyoda, *Carbon* **2003**, *41*, 2619 – 2624.
[9] J. P. R. Vissers, F. P. M. Mercx, S. M. A. M. Bouwens, V. H. J. D. Beer, R. Prins, *J. Catal.* **1988**, *114*, 291 – 302.
[10] H. Colin, G. Guiochon, *J. Chromatogr.* **1976**, *126*, 43 – 62.
[11] A. F. Bedilo, M. J. Sigel, O. B. Koper, M. S. Melgunov, K. J. Klabunde, *J. Mater. Chem.* **2002**, *12*, 3599 – 3604.
[12] T. Miyake, M. Hanaya, *J. Mater. Sci.* **2002**, *37*, 907 – 910.
[13] V. Narayanan, R. K. Thareja, *Modern Phys. Lett. B* **2003**, *17*, 121 – 129.
[14] M. Hirasawa, T. Seto, N. Aya, *J. Nanosci. Nanotechnol.* **2001**, *1*, 381 – 383.
[15] K. Hata, S. Yoshida, M. Fujita, S. Yasuda, T. Makimura, K. Murakami, H. Shigekawa, *J. Phys. Chem. B* **2001**, *105*, 10842 – 10846.
[16] R. K. Baldwin, K. A. Pettigrew, E. Ratai, M. P. Augustine, S. M. Kauzlarich, *Chem. Commun.* **2002**, 1822 – 1823.
[17] S. R. Kalidindi, S. B. Desu, *J. Electrochem. Soc.* **1990**, *137*, 624 – 628.
[18] T. A. Jurgens-Kowel, J. W. Rogers, *J. Phys. Chem. B* **1998**, *102*, 2193 – 2206.
[19] D. G. Kurth, T. Bein, *J. Phys. Chem.* **1992**, *96*, 6707 – 6712.
[20] C. Zheng, X. Zhang, S. He, Q. Fu, D. Lei, *J. Solid State Chem.* **2003**, *170*, 221 – 226.
[21] D. S. Su, R. Schlögl, *Catal. Lett.* **2002**, *83*, 3 – 4.
[22] L. Alexander, in *X-Ray Diffraction Procedures* (Ed.: H. Klug), Wiley, New York, **1962**, pp. 125.
[23] M. S. Dresselhaus, G. Dresselhaus, M. A. Pimenta, P. C. Eklund in *Analytical Application of Raman Spectroscopy* (Ed.: M. J. Pelletier), Blackwell Science, Oxford, **1999**, Chapter 9.
[24] V. G. Pol, M. Motiei, A. Gedanken, J. Calderon-Moreno, M. Yoshimura, *Carbon* **2004**, *42*, 111 – 116.
[25] V. G. Pol, S. V. Pol, Y. Gofer, J. Calderon-Moreno, A. Gedanken, *J. Mater. Chem.* **2004**, *14*, 966 – 969.
[26] M. Veith, N. Lecerf, S. Mathur, H. Shen, S. Hufner, *Chem. Mater.* **1999**, *11*, 3103 – 3112.
[27] A. Porporati, S. Roitti, O. Sbaizero, *J. Eur. Ceram. Soc.* **2003**, *23*(2), 247 – 251.
[28] J. J. Gallegos, T. L. Ward, T. J. Boyle, M. A. Rodriguez, L. P. Francisco, *Chem. Vap. Deposition* **2000**, *6*, 21 – 26.

Received: January 8, 2004
Published online: July 27, 2004

